

Transferability of Coarse Grained Potentials: Implicit Solvent Models for Hydrated Ions

Jia-Wei Shen,[†] Chunli Li,[‡] Nico F.A. van der Vegt,[‡] and Christine Peter^{*,†}

[†]Max Planck Institute for Polymer Research, Ackermannweg 10, D-55128 Mainz, Germany

[‡]Center of Smart Interfaces, Technische Universität Darmstadt, Petersenstrasse 32, D-64287 Darmstadt, Germany

 Supporting Information

ABSTRACT: Understanding the relation between structural and thermodynamic quantities obtained with simplified—e.g., coarse-grained (CG) or implicit-solvent—models is an ongoing challenge in the field of multiscale simulation. Assessing the transferability of such models to state points that differ from the one where the model was parametrized is important if one wants to apply these models to complex systems, which, for example, exhibit spatially varying compositions. Here, we investigate the transferability of CG (in this case implicit-solvent) ion models with effective pair potentials derived at very low concentrations to different ion concentrations in aqueous solution. We evaluate both thermodynamic and structural properties of systems of NaCl in aqueous solution both in atomistic explicit-solvent and CG simulations. For the explicit solvent simulations, osmotic coefficients have been calculated at a wide range of salt concentrations and agree very well with experimental data. It had been shown previously that a concentration-dependent dielectric permittivity can be used to make effective implicit-solvent pair potentials transferable since it accounts for the effect of ion concentration on solvent properties, resulting in very good osmotic properties of these models for a certain range of salt concentrations. We investigate the explicit and implicit solvent models also in terms of structural properties, where we can show how with a concentration-dependent dielectric constant one obtains very good structural agreement at low and intermediate salt concentrations, while for larger salt concentrations, multibody ion–ion correlations put a limit to straightforward transferability. We show how—guided by this structural analysis—the transferability of the implicit-solvent model can be improved for high ion concentrations. Doing so, we obtain transferable implicit-solvent effective pair potentials which are both structurally and thermodynamically consistent with an explicit solvent reference model.

1. INTRODUCTION

In simulations of complex molecular systems, reduced-resolution models have come to play a more and more important role due to the fact that highly detailed simulation methods (i.e., quantum or atomistic level simulations) can hardly handle the broad range of time and length scales involved. In most cases, coarse grained (CG) models are designed to merge groups of atoms into “superatoms”, i.e., CG beads, and the effective CG interaction potentials are derived by averaging over the microscopic details of models at higher resolution. In this way, CG methods reduce the number of degrees of freedom of the system and thus can speed up the simulations. In recent years, various approaches have been proposed to develop CG effective potentials,^{1–6} targeting thermodynamic properties^{7–11} or properties obtained from atomistic simulations of a reference system, the latter being either structural properties^{12–16} or mean forces.^{17–19} Unfortunately, CG models are dependent on the state point and system composition, and on most occasions, the transferability of these CG models to different state points (temperature, pressure, system composition, chemical environment, etc.) is poorly understood. Transferability of CG models is vitally important to the simulation of complex systems, where various complicated multi-body interactions are involved due to spatially biased structures and fluctuations. Yet, the construction of transferable CG models which accurately reproduce both structural and thermodynamic properties is an extremely challenging task, and the relation

between structural and thermodynamic properties of a CG model is central to many studies.^{20–22} Most often, effective pairwise potentials are used to describe the interactions in CG models. Since those effective pair potentials account for multibody effects, for example, three body interactions, they are only to a limited extent additive, and this sets limits to the transferability of the potentials. Understanding the physical nature of nonadditivity in the system of interest can help to make a CG model transferable. Many CG models presented in the literature were developed by constructing effective potentials in such a way that predominantly either structure or thermodynamic properties are reproduced, and then attempts were made to make the potentials transferable to similar systems (e.g., different concentration,²³ chain length,²⁴ component fraction,²⁵ etc.). In principle, transferability of effective pair potentials can be achieved in several ways: (i) One applies a model derived at/optimized for a given state point unaltered to a range of state points “nearby”; in that case, one has to carefully investigate the range in which this is permissible.¹⁵ (ii) One creates a new set of potentials for each state point one wants to investigate (e.g., density or temperature-dependent potentials).^{20,21,25,26} (iii) One specifically designs a single CG model with the aim to be transferable,^{19,27} or (iv) one uses a model derived at one state point and (analytically) modifies it to be applicable to different

Received: February 24, 2011

Published: April 27, 2011



conditions. (A simple example of the last case is the rescaling of potentials which one wants to apply to a different temperature.)

Recently, Villa et al. proposed a CG model for benzene/water.²² The CG benzene–benzene potential had been parametrized on the basis of the benzene–benzene potential of mean force of two benzene molecules in aqueous solution, i.e., at “infinite” dilution. By applying Kirkwood–Buff theory, they illustrate that this CG model can reproduce the changes in the benzene chemical potential and the activity coefficients of the mixtures over a range of mixture compositions (up to concentrations where benzene and water demix in the atomistic reference simulation). An explanation is that hydrophobic interactions between benzene solutes are short-ranged, and the multibody correlations involved in hydrophobic associations can be described by pairwise additive effective potentials (category i of the above list).

A different situation is found in the case of ion–ion interactions in aqueous solution. Due to long-range electrostatic interactions, the ions affect the behavior of water increasingly with increasing ion concentration. More specifically, the presence of many ions reduces the orientational fluctuations of the water molecules and thus the dielectric permittivity of the solvent. Therefore, effective ion–ion potentials parametrized at infinite dilution are not directly transferable to higher salt concentrations. Hess et al. developed a reduced-resolution (in this case implicit-solvent) potential for aqueous electrolyte solutions where an ion-concentration-dependent Coulomb term was added to the (ion-specific) pair interaction. Thus, by using a concentration-dependent dielectric permittivity of water, part of the multibody effects in the system were accounted for in the ion–ion pairwise interaction in the implicit solvent model.^{28–30} Their approach reproduced the NaCl solution osmotic properties and the ion coordination up to a concentration of 2.8 M (mol/L).

While in the case of the CG model of benzene–water mixtures²² the short-range hydrophobic interactions parametrized at infinite dilution were directly transferable to higher benzene concentrations, in the case of aqueous ion solutions, the ion–ion interactions determined at infinite dilution had to be split into a short ranged ion-specific and a long-range electrostatic part. The interactions were then made transferable by keeping the short-ranged part constant and analytically modifying the long-ranged electrostatic part (category iv of the above list).

On the basis of the work of Hess et al.,^{28,29} we revisit in this study the implicit solvent ion model with a concentration-dependent dielectric permittivity and investigate it in the context of transferability and structural and thermodynamic consistency of reduced-resolution models which are parametrized on the basis of an atomistic simulation model. To this end, we study osmotic coefficients and the structure of aqueous NaCl solutions over a wide range of concentrations. Osmotic properties of aqueous ion solutions have been investigated by several research groups on the basis of effective ion potentials and pair correlation functions.^{28–31} Luo and Roux³² presented a direct method to calculate the osmotic pressure of ion solutions by performing explicit-solvent atomistic simulations making use of a semipermeable wall. We employ this method by Luo and Roux to obtain osmotic coefficients of atomistic reference simulations of NaCl solutions. Thus, we can easily compare implicit and explicit solvent simulation results and evaluate our implicit solvent model. In addition, we also compare both atomistic and implicit solvent models with experimental measurements over a wide range of salt concentrations.

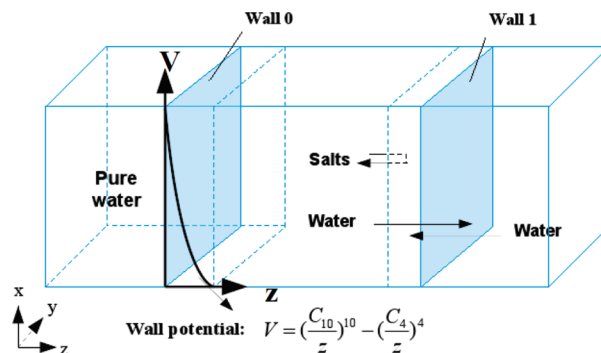


Figure 1. Setup of simulation systems to calculate the osmotic pressure of NaCl solutions using an explicit solvent model.

2. METHODS

2.1. Osmotic Pressure Calculation. Osmotic pressures of sodium chloride solutions were calculated at seven different concentrations, i.e., 0.5 m, 0.7 m, 1 m, 2 m, 3 m, 4 m, and 5 m (molality, mol/kg). Note that at the highest concentration of 5 m, this corresponds to only about 11 water molecules per ion pair. The atomic systems were set up in a similar way to Luo and Roux’s paper.³² In an orthorhombic simulation box, two semipermeable walls were imposed along the long axis *z* direction to restrict the ions within the central region of the box, while water molecules can go freely through the walls. The virtual walls were set up by modifying the wall functions built in GROMACS. Particularly, a 10–4 potential was shifted with a cutoff value in such a way that only repulsive forces can be felt by the ions as they start to diffuse out of the central region. The setup of the system with the NaCl solution and a pure water region is depicted in Figure 1. The entire system was subjected to *NpT* dynamics. The simulation box was set to be semi-isotropic, with the side lengths *x* and *y* fixed, and only the side length *z* was allowed to change. However, the distance between the two walls was fixed to ensure the volume of restricted ions to be constant. Therefore, the osmotic pressure of the salt solutions can be obtained by calculating the average forces exerted by the walls on the ions divided by the surface areas of the two walls.³² All of the atomistic systems were initially constructed using the program packmol,³³ by randomly placing a certain number of ions in the central region, while water molecules were distributed in the whole region of the orthorhombic box. In our osmotic pressure calculations, 11 112 water molecules were placed in the simulation box at each concentration. The number of ion pairs was chosen according to the concentration; i.e., 50, 70, 100, 200, 300, 400, and 500 ion pairs were put into the central region (see Figure 2) for concentrations of 0.5 m, 0.7 m, 1 m, 2 m, 3 m, 4 m, and 5 m, respectively. Then, a short minimization was performed, followed by an *NpT* simulation as long as 30 ns. The last 10 ns was block averaged and used to calculate the osmotic pressure. Figure 2 shows a snapshot of equilibrated structure using explicit solvent simulations to calculate the osmotic pressure of NaCl solutions at 4 m.

For each concentration, an independent *NpT* simulation of NaCl solution was performed for 20 ns before the calculation of osmotic pressure. This simulation includes a cubic periodic box filled with 5556 water molecules and an appropriate number of ion pairs according to the concentrations. One objective of this simulation is to calculate the volume of the central region

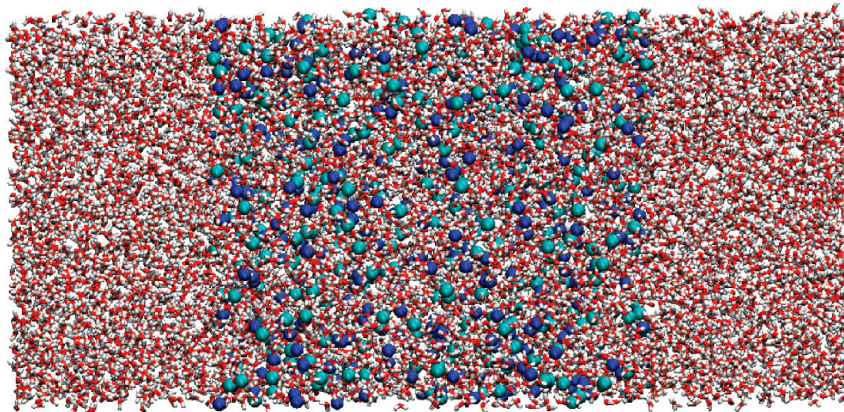


Figure 2. A snapshot of equilibrated structure using explicit solvent simulations to calculate the osmotic pressure of NaCl solutions at 4 m.

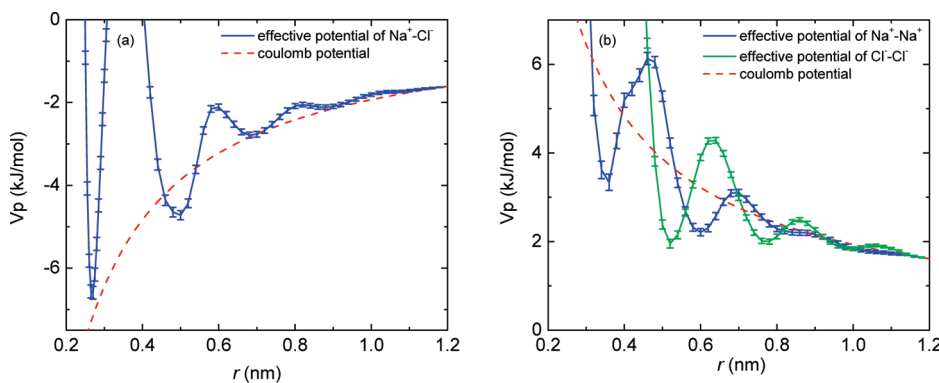


Figure 3. Effective potentials of (a) $\text{Na}^+ - \text{Cl}^-$ as well as (b) $\text{Na}^+ - \text{Na}^+$ and $\text{Cl}^- - \text{Cl}^-$ at infinite dilution derived from explicit solvent simulations. The red dashed line shows the Coulomb potential for $\epsilon_r = 71.9$ corresponding to SPC/E water. The (cumulative) errors in the PMF that originate from the errors of constraint force are also displayed.

restricting the ions in the following osmotic pressure calculations. Another is to derive the concentration-dependent dielectric permittivity $\epsilon_E(r)$, which will be mentioned in section 2.3.

2.2. Potentials of Mean Force and Effective Pair Potentials. Effective (implicit solvent/coarse grained) ion–ion pair potentials were derived as described in a previous study.^{28,29} Potentials of mean force (PMF) for all ion pairs ($\text{Na}^+ - \text{Cl}^-$, $\text{Na}^+ - \text{Na}^+$, and $\text{Cl}^- - \text{Cl}^-$) were computed using distance constraints, where the linear constraint solver (LINCS) algorithm³⁴ was used to keep two ions at a fixed distance. The free energy difference is then obtained by integrating the average constraint force f_c :

$$V(r_2) - V(r_1) = \int_{r_1}^{r_2} \langle f_c \rangle_r \, dr \quad (1)$$

In our simulations, we are limited to finite distances and therefore integrate backward starting from a distance $r_m = 1.2 \text{ nm}$. Since the effective potential is very close to a Coulomb interaction between 1.0 and 1.2 nm,^{28,29} the total effective potential can be expressed as

$$V_p(r) = \begin{cases} \int_{r_m}^r \left[\langle f_c \rangle_s + \frac{2k_B T}{s} \right] ds + \frac{q_1 q_2}{4\pi \epsilon_0 \epsilon_r r_m} & r < r_m \\ \frac{q_1 q_2}{4\pi \epsilon_0 \epsilon_r r} & r \geq r_m \end{cases} \quad (2)$$

where $(2k_B T)/s$ is an entropic term, k_B is the Boltzmann

constant, and T is the temperature. ϵ_0 and ϵ_r are the dielectric permittivity of the vacuum and of the SPC/E water model, respectively. If one subtracts the (long-range) Coulombic interactions between different ions from $V_p(r)$ in eq 2 one obtains the short-range (non-Coulombic) contribution to the interaction between these ions:

$$V_{\text{short}}(r) = V_p(r) - V_{\text{coul}}(r) = V_p(r) - \frac{q_1 q_2}{4\pi \epsilon_0 \epsilon_r r} \quad (3)$$

This short-range contribution $V_{\text{short}}(r)$ is used as tabulated ion-specific pair interaction in combination with Coulomb interactions (which are typically computed using Particle Mesh Ewald summation or similar) in implicit solvent/coarse grained ion simulations.

A series of independent constrained simulations for the $\text{Na}^+ - \text{Cl}^-$, $\text{Na}^+ - \text{Na}^+$, and $\text{Cl}^- - \text{Cl}^-$ ion pairs were carried out at distances up to 1.2 nm. For like-ion pairs, intervals of 0.02 nm between constraint distances were used. For the $\text{Na}^+ - \text{Cl}^-$ pair, intervals of 0.005 nm were used between 0.2 and 0.4 nm to get sufficient sampling around the first minimum of the potential, and intervals of 0.02 nm were used above 0.4 nm. All systems contained two ions and 1000 water molecules in a dodecahedron box. Figure 3 shows the effective potentials of $\text{Na}^+ - \text{Cl}^-$ (left panel) as well as $\text{Na}^+ - \text{Na}^+$ and $\text{Cl}^- - \text{Cl}^-$ (right panel) at infinite dilution and, for comparison, the Coulomb

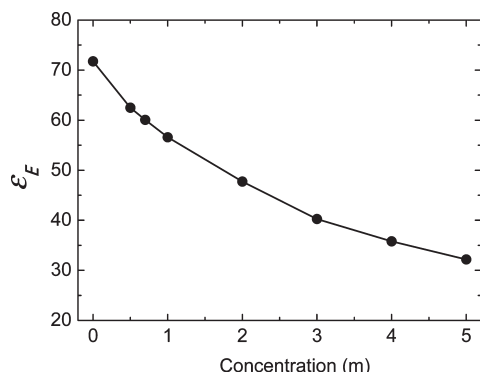


Figure 4. The equilibrium concentration dependent dielectric permittivity ϵ_E as a function of NaCl concentrations, calculated from explicit solvent simulation of SPC/E water model.

interaction for a dielectric constant of $\epsilon_r = 71.9$ (SPC/E water model).

2.3. Concentration-Dependent Dielectric Constants. The potentials of mean force determined as described in the above paragraph—which by construction include the effect of the solvent on the ion–ion interactions—can be used as effective pair potentials for ions in implicit solvent simulations. However, at finite concentrations of aqueous NaCl solutions, water molecules will feel the fields of several ion pairs at the same time, and their orientational fluctuations will be suppressed. It has been found that this effect becomes important for NaCl solutions with a concentration above 0.5 M,^{28,30} and it would lead to a breakdown of additivity of effective ion potential based on the potentials of mean force (an additional effect of multi-ion correlations will be discussed later in the paper). The effect of the ion concentration on the water molecules can be accounted for with an ion-concentration-dependent dielectric permittivity $\epsilon_E(c)$.^{28,29} We determined $\epsilon_E(c)$ (of the water molecules) at concentrations of 0.5 m, 0.7 m, 1 m, 2 m, 3 m, 4 m, and 5 m via explicit solvent simulations from the fluctuations of the total dipole moment of the solvent molecules.³⁵ Simulations at 1 m, 2 m, 3 m, 4 m, and 5 m were performed for 20 ns. For the concentrations of 0.5 m and 0.7 m, simulations were performed for 40 ns. ϵ_E as a function of salt concentration is displayed in Figure 4. It is not surprising that ϵ_E decreases with the increasing salt concentration because the orientational fluctuations of water become smaller at higher salt concentrations. Our results agree well with previous simulations by Hess et al.²⁹ and Kalcher and Dzubiella.³⁰ For all concentrations, the atomistic simulations slightly overestimate the effect of adding salt to the solutions; i.e., compared to experimental results, the dielectric constant is slightly too low, with a maximum deviation of 13%.

The concentration-dependent dielectric permittivity can be used to correct the effective ion–ion interaction potentials over the whole range for the dependence on the salt molality c :²⁸

$$\begin{aligned} V_{\text{total}}(r, c) &= V_{\text{short}}(r) + V_{\text{coul}}(r, c) \\ &= V_{\text{short}}(r) + \frac{q_1 q_2}{4\pi\epsilon_0\epsilon_E(c)r} \end{aligned} \quad (4)$$

The dielectric permittivity dependent effective potentials in eq 4 were applied to the implicit solvent simulations, with the $\epsilon_E(c)$ calculated from explicit solvent simulations.

3. COMPUTATIONAL DETAILS

3.1. Explicit Solvent Simulations. All explicit solvent simulations were carried out using molecular dynamics simulation package GROMACS 4.0.7.³⁶ Simulations were performed under constant temperature T (298 K) and pressure P (1 bar) conditions using a Berendsen thermostat and a Berendsen barostat³⁷ with a coupling time of 0.1 ps. Particle Mesh Ewald (PME)³⁸ was applied to treat the electrostatic interactions with a grid spacing of 0.12 nm, a PME order of 4, and a real space cutoff of 0.9 nm. On the other hand, the cutoff distance of Lennard-Jones interactions was set as 0.9 nm. In addition, long-range dispersion correction was applied for energy and pressure. The integration time step was set as 4 fs, and the neighbor list was updated every five steps.

The SPC/E model was used for water molecules in all explicit solvent simulations, with bond lengths and angles constrained using the SETTLE algorithm.³⁹ On the other hand, the parameters of Lennard-Jones potentials for Na^+ and Cl^- were taken from the Kirkwood–Buff force field (KBFF) presented in the paper of Weerasinghe and Smith.⁴⁰ The geometric combination rule was used for van der Waals interactions between different types of atoms in the system. However, a scaling factor of 0.75 was added to the interactions between the cations and oxygen atoms in water molecules, as presented in the paper of Weerasinghe and Smith.

3.2. Implicit Solvent Simulations. In all implicit solvent simulations, stochastic dynamics with a friction coefficient of 1.0 ps^{-1} was used, and these simulations were performed in the NVT ensemble with the average volume of corresponding explicit solvent simulations. The initial structures of the implicit simulation at various concentrations were derived from the final structure of the corresponding explicit solvent simulations. By using the effective potentials between ions in the implicit solvent simulation, the solvent degrees of freedom are averaged, and the osmotic coefficient of NaCl solution at various concentrations could be calculated:

$$\phi = \frac{P}{P_{\text{ideal}}} = \frac{K - \Xi}{K} \quad (5)$$

where K is the kinetic energy and Ξ is the virial of the ions.²⁹

3. RESULTS AND DISCUSSION

In the present work, we evaluate the transferability of the implicit solvent ion (NaCl) model from parametrization at infinite dilution to a wide range of concentrations, from 0.5 m to 5 m. To this end, we study the correspondence with atomistic reference simulations in terms of both structural as well as thermodynamic properties, in this case, the osmotic coefficient, a thermodynamic quantity which is sensitively related to the structure of the solution. It is a measure of the strength of the effective interactions between ions in solution and depends sensitively on the ion–ion coordination. At first, we compare osmotic coefficients of NaCl solutions obtained from explicit-solvent atomistic simulations (converting osmotic pressures to osmotic coefficients via $\Phi = P/P_{\text{ideal}}$; see eq 5) and from implicit solvent simulations with experimental data,⁴¹ as shown in Figure 5. One can see that the force field parameters we used in explicit solvent simulations are able to reproduce the experimental osmotic coefficient accurately over a wide range of salt concentrations, especially below 4 m. This is consistent with the

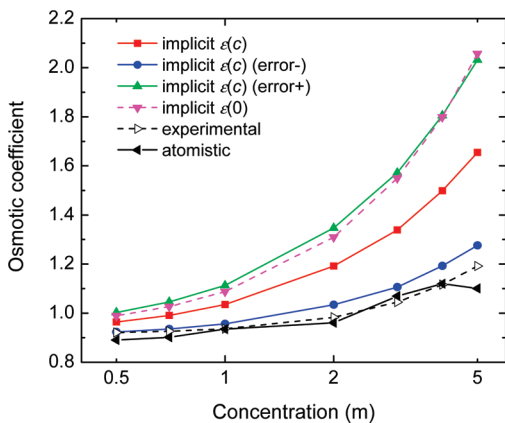


Figure 5. Osmotic coefficients of NaCl solutions from the explicit solvent model (black full triangles), from the implicit solvent model with a concentration-dependent dielectric constant (red full squares, label “implicit $\epsilon(c)$ ”), the implicit solvent with a pure water dielectric constant (pink full triangles, dashed line, label “implicit $\epsilon(0)$ ”), as well as experimental data (empty black triangles).⁴¹ The osmotic coefficients computed with effective potentials using error estimation (as discussed in the text; green and blue symbols, denoted as “implicit $\epsilon(c)$ (error+)” and “implicit $\epsilon(c)$ (error-)”, respectively) are also displayed.

previous study^{28,42} that this force field could reproduce the experimental results^{41,43} for osmotic coefficients and activity coefficients. The concentration-dependent implicit solvent model reproduces the general behavior of the osmotic coefficient compared with the atomistic simulations, although we should note that with increasing ion concentration the deviation becomes larger—and between ~ 0.75 m and ~ 3 m one finds a qualitative disagreement. Here, the implicit-solvent osmotic coefficient is greater than 1, whereas it is less than 1 in the atomistic simulations; i.e., the osmotic pressure of the implicit solvent system is greater than that of an ideal solution, while the atomistic/experimental osmotic pressures are smaller than that of an ideal solution. We will discuss the correspondence between implicit solvent and explicit solvent osmotic pressures again later in this paper, where we will show that these implicit solvent osmotic coefficients are extremely sensitive to tiny changes in the ion–ion interaction potential. The results of the implicit solvent ion model agree well with the work of Kalcher and Dzubiella,³⁰ where osmotic coefficients of atomistic simulations were computed with ion potentials of mean force and concentration dependent dielectric constant via a virial route. To illustrate the effect of the concentration dependent $\epsilon_E(c)$ on the implicit solvent model, the osmotic coefficients of uncorrected (with permittivity of pure SPC/E water) implicit solvent simulations are also displayed in Figure 5 (dashed pink line). For these simulations with the dielectric constant of SPC/E water, we will from now on use the label “implicit $\epsilon(0)$ ” while we will label the model with concentration-dependent dielectric constant “implicit $\epsilon(c)$ ”. At all concentrations, the “implicit $\epsilon(0)$ ” model predicts substantially larger osmotic coefficients than the “implicit $\epsilon(c)$ ” model, with the difference growing with increasing ion concentration.

One might argue that the increasing deviation between the “implicit $\epsilon(c)$ ” model and the atomistic simulations mainly results from multi-ion effects which should become more prominent with increasing ion concentration and which are not captured by a concentration dependent $\epsilon_E(c)$. To investigate this more closely, we estimated the magnitude of various sources for

errors in the osmotic coefficients in the implicit solvent simulations. We first estimate the error in the kinetic energy and the virial which enter eq 5—including the influence of the thermostat settings on the kinetic energy. The accuracy of the osmotic coefficient computation is 0.002 for 0.7 m and 0.001 for the remaining concentrations. The accuracy is much higher than the osmotic coefficient differences between atomistic and CG levels of resolution. A more important source of error is the accuracy of the PMF calculation. The PMF for all ion pairs ($\text{Na}^+–\text{Cl}^-$, $\text{Na}^+–\text{Na}^+$, and $\text{Cl}^-–\text{Cl}^-$) were obtained by integrating the average constraint force at a large number of ion distances. The error in the average constraint force accumulates to an error in the resulting PMF indicated in Figure 3. As the osmotic coefficient is very sensitive to the ion parameters or the effective potentials, the cumulative errors in the PMF may have remarkable influence on the osmotic coefficient of the implicit solvent model. To estimate the magnitude of this, we computed two limiting cases, a PMF– (PMF minus the error at each point) and a PMF+ (PMF plus the error at each point) for each of the three ions pairs ($\text{Na}^+–\text{Cl}^-$, $\text{Na}^+–\text{Na}^+$, and $\text{Cl}^-–\text{Cl}^-$) and determined the respective short-range (tabulated) potentials (V_{short} , eq 3). With these “error estimated” effective potentials, we performed implicit solvent simulations (again with concentration-dependent dielectric constant) and determined the osmotic coefficients. The results are shown in Figure 5 (indicated as “implicit $\epsilon(c)$ (error+)” and “implicit $\epsilon(c)$ (error-)”). We are aware that this procedure is not a stringent estimation of the error of the osmotic coefficients; nevertheless, it nicely illustrates that even a small error (the PMF calculations had been carried out very accurately) in the pair potentials of mean force between the two ions may have a very big effect on the osmotic behavior of the implicit solvent model. The “implicit $\epsilon(c)$ (error+)” and “implicit $\epsilon(c)$ (error-)” models are slight variations (within the error bars of the underlying potentials of mean force) of the “implicit $\epsilon(c)$ ” model which are slightly less or more attractive over the entire range of the short-range potential V_{short} . It is interesting that the osmotic coefficients obtained from the “implicit $\epsilon(c)$ (error-)” simulations are very close to the atomistic and experimental results at all concentrations up to 4 m, while the osmotic coefficients of the “implicit $\epsilon(c)$ (error+)” simulations are very close to those obtained with the uncorrected “implicit $\epsilon(0)$ ” model. This finding shows that the osmotic coefficient is a highly sensitive thermodynamic property, and in implicit-solvent ion models it strongly depends on the ion–ion effective potentials. It also shows that it is difficult to assess the quality of a CG ion model on the basis of osmotic behavior alone, since for example the “implicit $\epsilon(c)$ (error+)” and the uncorrected “implicit $\epsilon(0)$ ” models exhibit almost the same osmotic behavior but for completely different reasons and with very different consequences on structural properties, as we will show below. Here, we would like to point out that even though the osmotic coefficient alone might not be a good measure to assess the agreement with the underlying atomistic model, it is nevertheless a crucial property in force field parametrization. The osmotic behavior strongly depends on the ion types, and ion specific force fields (both with explicit and implicit solvent) should reproduce these differences between the ions.

The osmotic coefficient is closely linked to the structure of the ion solution (see, e.g. ref 30); thus we compared the structural properties obtained in the explicit and implicit solvent (“implicit $\epsilon(c)$ ” and “implicit $\epsilon(0)$ ”) simulations. Figure 6 shows the radial distribution functions (RDFs) between Na^+ and Cl^- in these

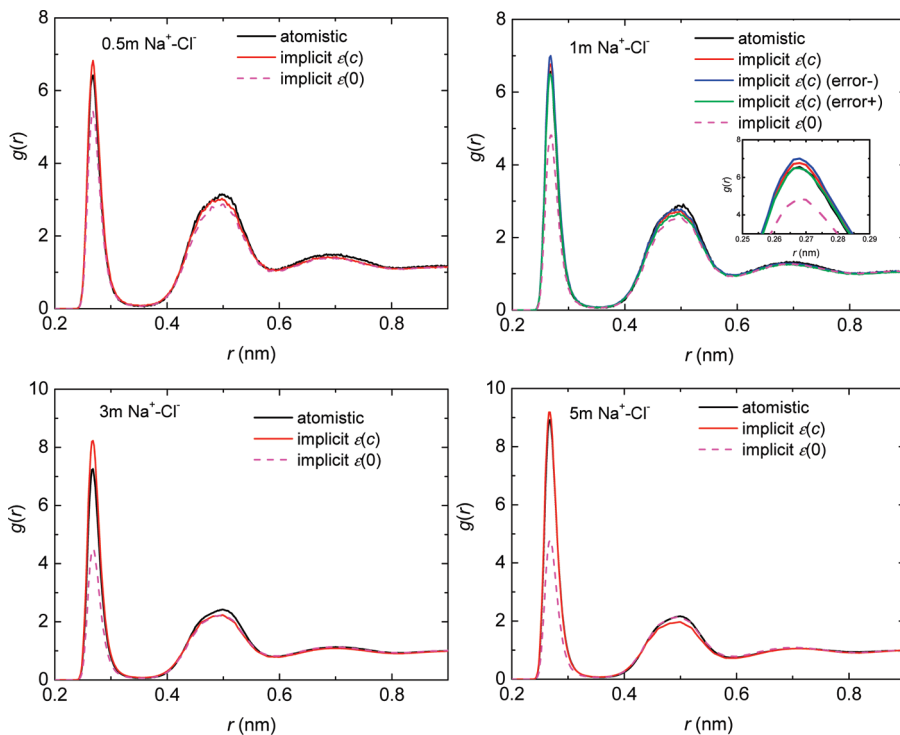


Figure 6. The radial distribution functions (RDFs) of $\text{Na}^+ - \text{Cl}^-$ in explicit, implicit and uncorrected implicit solvent simulations at different concentrations. The RDF of $\text{Na}^+ - \text{Cl}^-$ from computation with effective potentials using the error estimate of the potentials of mean force (denoted as “implicit $\varepsilon(c)$ (error−)” and “implicit $\varepsilon(c)$ (error+)”; see text) for 1 m is also displayed.

Table 1. The $\text{Na}^+ - \text{Cl}^-$ Coordination Numbers in the Contact Minimum (0–0.35 nm) and the Solvent Shared Minimum (0.35–0.59 nm) for Explicit Solvent Simulations and Simulations with the “implicit $\varepsilon(c)$ ” and “implicit $\varepsilon(0)$ ” Models

	explicit	0.00–0.35 nm				0.35–0.59 nm				
		implicit $\varepsilon(c)$	relative difference (%)	implicit $\varepsilon(0)$	relative difference (%)	explicit	implicit $\varepsilon(c)$	relative difference (%)	implicit $\varepsilon(0)$	relative difference (%)
0.5 m	0.053	0.056	5.7	0.045	15.1	0.359	0.349	2.8	0.329	8.4
0.7 m	0.079	0.079	0.0	0.060	24.1	0.489	0.461	5.7	0.435	11.0
1 m	0.106	0.111	4.7	0.080	24.5	0.648	0.622	4.0	0.584	9.9
2 m	0.212	0.233	9.9	0.148	30.2	1.149	1.094	4.8	1.051	8.5
3 m	0.337	0.382	13.4	0.217	35.6	1.580	1.499	5.1	1.488	5.8
4 m	0.492	0.528	7.3	0.291	40.9	1.950	1.823	6.5	1.897	2.7
5 m	0.656	0.669	2.0	0.367	44.1	2.262	2.111	6.7	2.280	0.8

simulations at concentrations of 0.5 m, 1 m, 3 m, and 5 m. At relatively low concentrations of 0.5 m and 1 m, the first peaks (contact ion pairs) of the “implicit $\varepsilon(c)$ ” $\text{Na}^+ - \text{Cl}^-$ RDFs agree very well with explicit solvent simulations, while the second peaks (solvent shared ion pairs) are slightly lower compared to explicit solvent simulations. The effect of the concentration dependent permittivity can be best seen by comparing to the implicit solvent simulations with the permittivity of pure SPC/E water (“implicit $\varepsilon(0)$ ” model), shown by the dashed magenta lines in Figure 6, which severely underestimate the first peaks of the $\text{Na}^+ - \text{Cl}^-$ RDFs.

In Table 1, we show the $\text{Na}^+ - \text{Cl}^-$ coordination numbers in the contact minimum (0–0.35 nm) and the solvent shared minimum (0.35–0.59 nm) for explicit, corrected, and uncorrected implicit solvent simulations, which give a quantitative description of the structure information of NaCl solution at

different concentrations. These numbers quantify the qualitative observation made above, that the structural agreement between the explicit solvent and implicit solvent models is good after using a concentration-dependent dielectric constant. The uncorrected “implicit $\varepsilon(0)$ ” model, where the larger dielectric permittivity weakens the interaction between Na^+ and Cl^- ions, severely underestimates the coordination numbers of the first peak at all concentrations, and this effect becomes stronger with an increase in concentration. For the second peak in the RDF, these effects are much weaker. Overall, these results confirm that the use of a concentration-dependent dielectric constant $\varepsilon_E(c)$ makes the implicit solvent model which had been parametrized at infinite dilution transferable to a wide range of concentrations.

Figure 6 (for 1 m concentration) and Figure S1 in the Supporting Information show the $\text{Na}^+ - \text{Cl}^-$ RDFs obtained with the “implicit $\varepsilon(c)$ (error+)” and “implicit $\varepsilon(c)$ (error−)”

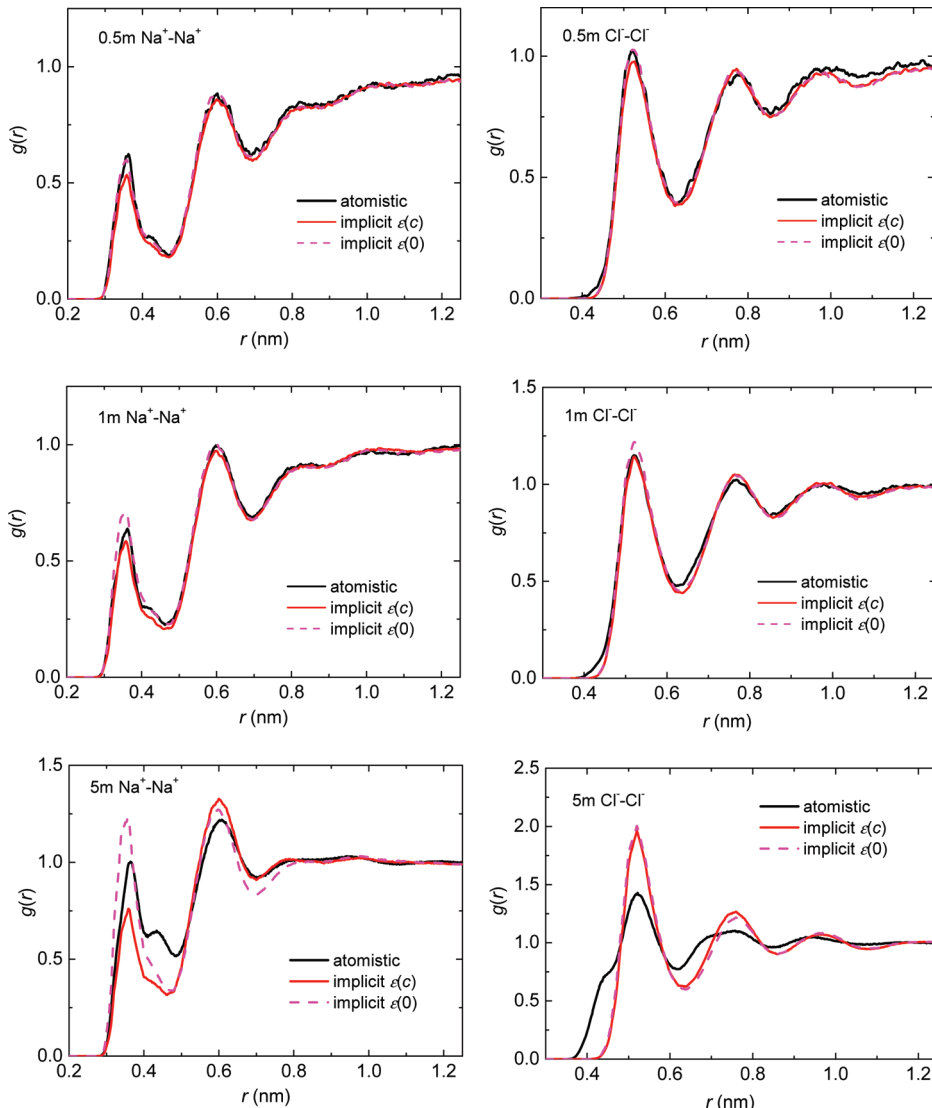


Figure 7. The radial distribution functions of Na^+-Na^+ and Cl^--Cl^- in explicit, implicit, and uncorrected implicit solvent simulations at 0.5 m, 1 m, and 5 m concentrations of NaCl solutions (labels and line colors as in previous figures).

models. Note that despite the fact that the osmotic coefficients from these models are drastically different (see Figure 5), the structure appears to be hardly affected while the uncorrected “implicit $\epsilon(0)$ ” (which leads to similar osmotic coefficients as “implicit $\epsilon(c)$ (error+)”) gives a rather different structure, especially in the first coordination shell. These observations show that even though the osmotic coefficient is intimately linked to the electrolyte structure (see Kalcher and Dzubiella³⁰) and can be reproduced by a structure-based (i.e., pair-PMF based) implicit solvent model, it is very sensitive to errors in the PMF. In our particular example, we have mimicked a systematic error by generating—within the error bars of the PMF calculation—slightly more attractive (model “implicit $\epsilon(c)$ (error-)”) or slightly more repulsive (model “implicit $\epsilon(c)$ (error+)”) interaction potentials. The simulations with these modified interaction potentials show that reproducing electrolyte structure and a related thermodynamic property such as the osmotic coefficient may depend differently on different aspects of the interaction potential, namely, the short-ranged attraction in the different minima of V_{short} versus the overall attraction which is dominated

by the tail of the potentials (mainly electrostatic interaction). This is confirmed if one looks at the Kirkwood–Buff integral, i.e., the integrated ion–ion radial distribution function (with all ions treated as indistinguishable)—a property that establishes the link between osmotic behavior, association, and structure (data shown and in more detail discussed in the Supporting Information). For this property, we see a correspondence between the different implicit solvent electrolyte models and the atomistic simulations, which is very similar to the osmotic coefficient.

The above results also show that it is possible to obtain equally good structural agreement, in this case, a good representation of the electrolyte structure, with different potentials—even though they lead to different thermodynamic behaviors. This is an important observation in the context of transferability of reduced resolution models since the aim of a well transferable model is often not in perfect agreement with a reference at a single state point but rather in reasonable agreement (both structurally and thermodynamically) for a range of state points. The results in the “implicit $\epsilon(c)$ (error \pm)” models show that this can in principle be achieved without entirely sacrificing structural agreement.

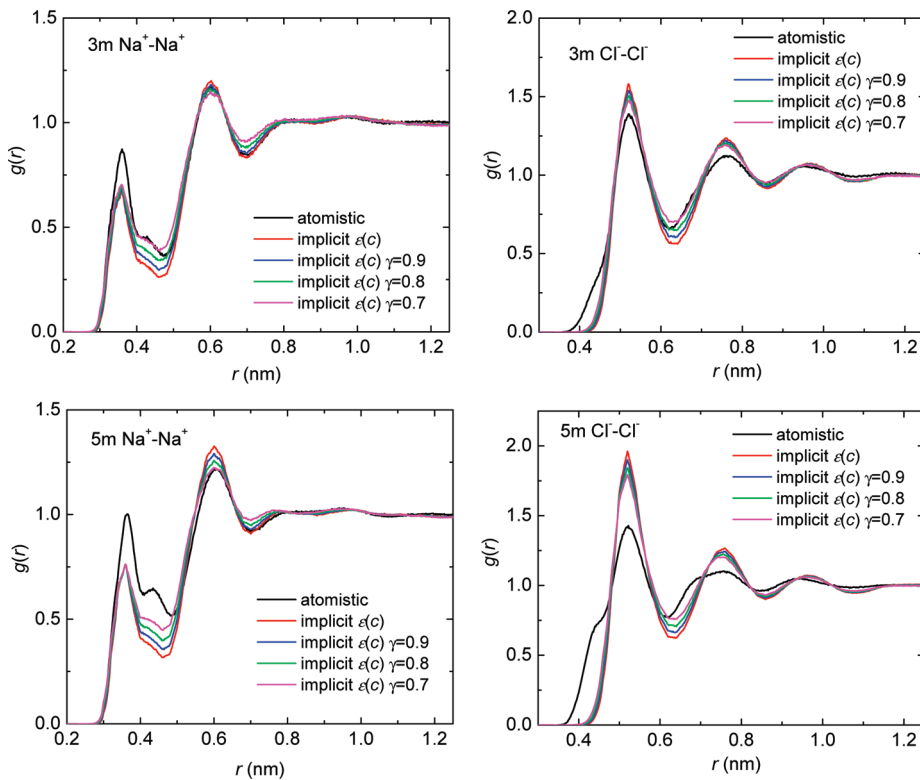


Figure 8. Radial distribution functions of Na^+-Na^+ and Cl^--Cl^- in explicit, “implicit $\epsilon(c)$ ”, and PMF-scaled implicit solvent simulations at 3 m and 5 m concentrations of NaCl solutions. Scaling factors γ of 0.9, 0.8, and 0.7 were used.

As discussed above, the deviations of the osmotic coefficient obtained by the implicit solvent model from the explicit solvent reference keeps increasing with the increasing concentration (even for the “implicit $\epsilon(c)$ (error–)” set of potentials which reproduces the atomistic osmotic coefficients at low concentrations very well). They are most likely due to higher order ion–ion correlations which are not captured by a concentration-dependent $\epsilon_E(c)$, which only accounts for the changes in the solvent behavior with increasing ion concentration. To better understand this, we investigated the structure of like-charged ion pairs, i.e., Na^+-Na^+ and Cl^--Cl^- RDFs, in explicit and all implicit solvent models, which are displayed in Figure 7 and Figure S2 (in the Supporting Information) for selected concentrations. It is not surprising that at the relatively low concentrations of 0.5 m and 1 m, both Na^+-Na^+ and Cl^--Cl^- RDFs show good agreement between explicit and implicit solvent simulations. At higher concentrations (see, for example, the 5 m case), the implicit solvent model (“implicit $\epsilon(c)$ ”) underestimates the first peak and overestimates the second peak of the Na^+-Na^+ RDF, and the Cl^--Cl^- RDF is overstructured compared to the explicit solvent reference. In the explicit solvent reference, the Cl^--Cl^- RDF exhibits a shoulder before the first peak at 5 m, which indicated that at these high concentrations, special configurations (most probably involving more than two ions) start to play an important role. Since these configurations had not been accounted for in the parametrization of the implicit solvent model, they can hardly be reproduced and set a limit to what we can expect in terms of transferability of the model to higher concentrations. Figure 7 also displays the like-ion RDFs for implicit solvent simulations with the permittivity of pure water, which shows that the transition from $\epsilon_E(0)$ to $\epsilon_E(c)$ has a different effect on the Na^+-Na^+ and Cl^--Cl^- structures (also

compared to the Na^+-Cl^- structure). The Cl^--Cl^- structure is hardly affected by the change in dielectric constant, while the first peak of the Na^+-Na^+ structure is strongly affected (we provide tables with the corresponding coordination numbers in the Supporting Information). Since we know already that the dielectric constant has a strong effect on Na^+-Cl^- (contact) pairs, these results indicate that for higher concentrations the Na^+-Na^+ structure is influenced by higher order ion correlations involving more than two ions, possibly including Cl^- ions.

The RDF of like ions reflects the fact that reducing the dielectric permittivity accounts for the change in solvent properties; i.e., the long-range attractive interactions need to be adapted accounting for the reduced dielectric screening by the water. At low ion concentrations, this is sufficient, and the effective ion–ion potentials are perfectly additive and transferable. The biggest effect of the reduced screening will be on the close (oppositely charged) contact ion pairs, i.e., the first peak in the Na^+-Cl^- RDFs (as observed in Figure 6). One could however argue that for like-charged ion pairs one would rather expect a reduced repulsion at higher concentrations because of multi-ion correlations (mediated interactions through nearby counterions, for example). When these multibody effects between the ions start to play a role, direct pairwise additivity of the effective potentials breaks down. The reduced ion–ion repulsion at short distances would be an effect that counteracts the reduced dielectric screening when using $\epsilon(c)$, which explains why the “implicit $\epsilon(0)$ ” shows a different behavior for the first peak of the Na^+-Na^+ RDF compared to the “implicit $\epsilon(c)$ ” (see Figure 7). Therefore, the explicit hydration effects of ions within short range at high concentrations cannot be simply described by only applying a concentration-dependent dielectric constant

$\varepsilon_E(c)$, and we probably need a second parameter to take effects on $\text{Na}^+–\text{Na}^+$ and $\text{Cl}^-–\text{Cl}^-$ interactions into account.

In the following, we will describe two possible approaches (which we will label “PMF-scaled” and “RDF-refined”) to improve the transferability of the implicit solvent electrolyte model to very

Table 2. Osmotic Coefficients of NaCl Solutions at 3 m and 5 m Concentrations Calculated from Explicit Solvent and Different Implicit Solvent Simulations (“implicit $\varepsilon(c)$ ”, “PMF-scaled” ($\gamma = 0.8$), and “RDF-refined” as Described in the Text)

	explicit	implicit	PMF-scaled	RDF-refined
0.5 m	0.890	0.964		0.939
1 m	0.935	1.035		0.988
3 m	1.069	1.339	1.060	1.204
5 m	1.101	1.654	1.190	1.427

high concentrations. In the first approach, denoted as “PMF-scaled”, we made an attempt to adapt the (short-range) interaction between $\text{Na}^+–\text{Na}^+$ and $\text{Cl}^-–\text{Cl}^-$ pairs since—as discussed above—the repulsion between like ions at short distances in solutions at high concentration is possibly reduced (compared to lower concentrations). This we did by scaling (down) the PMF that is the basis of the effective pair potential by a factor γ (we will discuss other possibilities to reduce the like-ion repulsion below). Figure 8 displays the RDF of $\text{Na}^+–\text{Na}^+$ and $\text{Cl}^-–\text{Cl}^-$ pairs in explicit, normal “implicit $\varepsilon(c)$ ”, and PMF-scaled implicit solvent simulations at concentrations of 3 m and 5 m. Scaling factors γ for both $\text{Na}^+–\text{Na}^+$ and $\text{Cl}^-–\text{Cl}^-$ PMFs in the range of 0.9 to 0.7 were used. This new model with reduced short-range repulsion between like-charged ion pairs shows only a slightly better agreement of the $\text{Na}^+–\text{Na}^+$ and $\text{Cl}^-–\text{Cl}^-$ RDFs with the explicit solvent simulations (see Figure 8).

The $\text{Na}^+–\text{Cl}^-$ RDFs are not affected at all by the change (data not shown). More importantly, these modifications have a

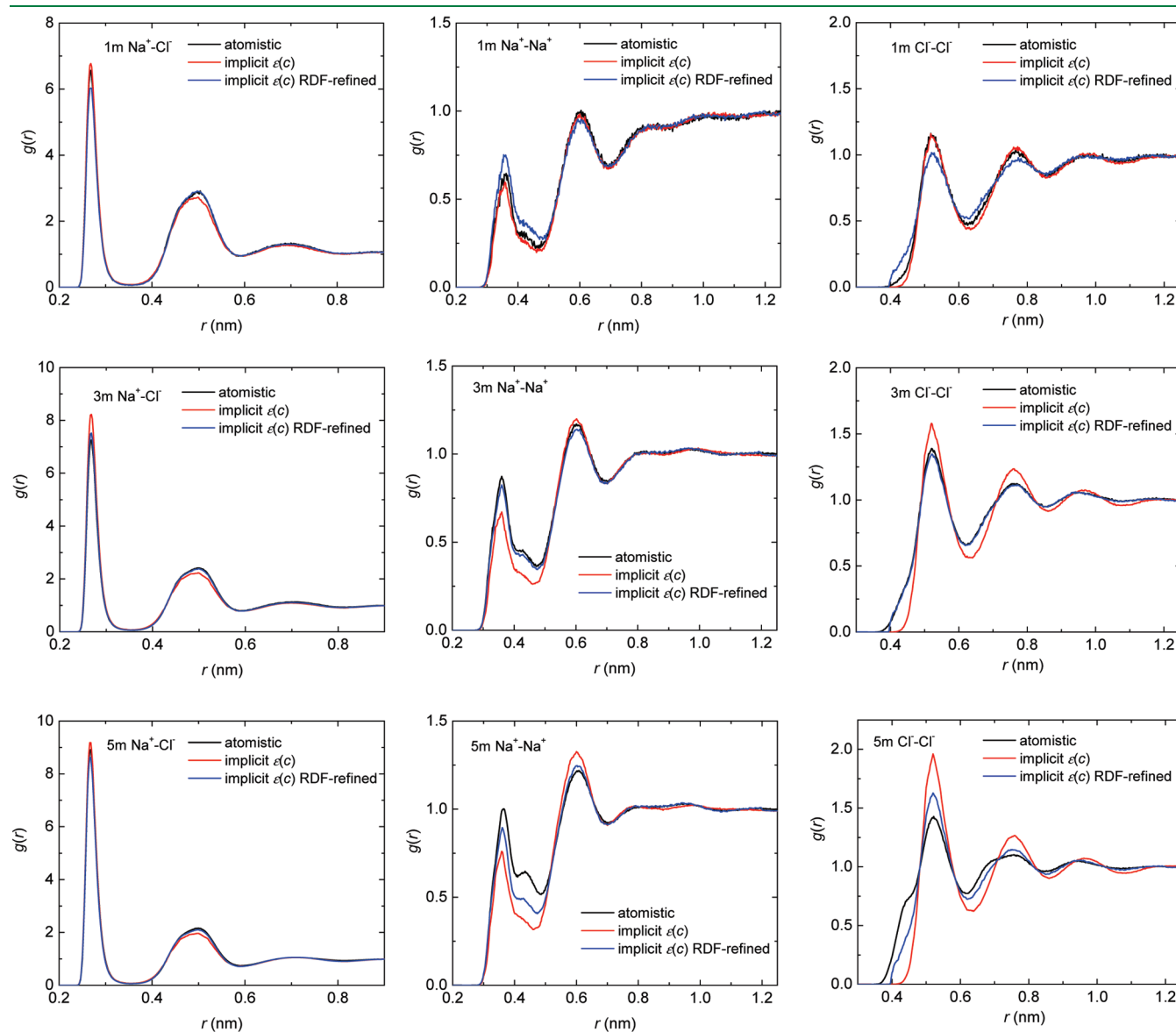


Figure 9. Radial distribution functions of $\text{Na}^+–\text{Cl}^-$, $\text{Na}^+–\text{Na}^+$, and $\text{Cl}^-–\text{Cl}^-$ in explicit, “implicit $\varepsilon(c)$ ”, and “RDF-refined” implicit solvent simulations at 1 m, 3 m, and 5 m concentrations of NaCl.

large effect on the osmotic behavior of the system, reducing the osmotic coefficient and bringing it much closer to the values of the atomistic simulations, as can be seen in Table 2. In fact, the osmotic coefficient can be used to determine the optimal choice for the exact value of the scaling parameter γ . In our case, $\gamma = 0.8$ gives the best fit of atomistic osmotic coefficient at 3 m and 5 m. By rescaling the entire PMF before splitting the interaction into a short-range and a long-range electrostatic part (eq 3), we have reduced the overall repulsion in the range of the short distances (while the long-range Coulomb interactions beyond the cutoff remain as before). This appears to be a quite ad hoc approach to account for multi-ion correlation, and we are aware that we showed already that the osmotic coefficient alone is a weak criterion for a good model. Nevertheless, we show that we can employ this ad hoc but physically justifiable additional parameter to improve the osmotic behavior at high ion concentrations without corrupting the structural properties of the model. Alternative to the above approach, we tried two other scaling methods, thus providing three possible ways of modifying the ion–ion repulsion of like ion pairs: (i) We have reduced only the short-range interaction V_{short} (scaled the tabulated potential). (ii) We have reduced only the Coulombic contribution (repulsion) to the interaction between like ions. (iii) We have reduced the short-range total interaction. The latter is done by scaling the PMF as described above. It appears that the PMF scaling gives the best results among these attempts, both structure-wise and in terms of osmotic coefficient. With this additional (rather arbitrary but physically justifiable) scaling factor, the implicit solvent ion potentials could be made transferable over the entire range of concentrations, giving a good correspondence between atomistic reference and implicit solvent simulations both in terms of structure and osmotic coefficient.

One might argue that with these scaling parameters one ends up reparameterizing the implicit solvent model for higher concentrations. However, as opposed to generating a series of independent models for each state point, this approach uses in principle the same potentials as before, which consist of a short-range/ion-specific part and (concentration dependent) long-range Coulomb interactions, and just modifies the strength of these interactions accordingly to account for multibody effects.

In a second approach to make the “implicit $\epsilon(c)$ ” model transferable to very high concentrations, we focus on the structure of the like-charged ion pairs since these RDFs appear to be most affected by the limited transferability of the model (see Figure 7), even for models with correct osmotic behavior (see Figure 8). Following the “structure-based” coarse graining methodology,^{12,44} we refine the ion–ion interactions by taking the electrolyte structure from atomistic simulations as a reference. Iterative methods such as iterative Boltzmann inversion (IBI) or inverse Monte Carlo (IMC) are methods that refine CG potentials such that radial distribution functions of the reference system are reproduced.^{12,44} Here, we do not iteratively refine the $\text{Na}^+–\text{Cl}^-$, $\text{Na}^+–\text{Na}^+$, and $\text{Cl}^-–\text{Cl}^-$ potentials until the respective radial distribution functions are exactly reproduced. Instead, we employ a single refinement step where we adjust the concentration-dependent implicit solvent model at 3 m to better reproduce the corresponding RDFs. That means we add a correction term to V_{short} that accounts for the difference in the RDF obtained with the implicit solvent model ($g^{\text{“implicit } \epsilon(c)}(r)$) compared to the reference RDF ($g_{\text{ref}}(r)$). This correction term is $kT \ln(g^{\text{“implicit } \epsilon(c)}(r)/g_{\text{ref}}(r))$. This new set of potentials, from now on labeled as “RDF-refined”, which is based on the pair

PMFs at infinite dilution and refined at 3 m concentration, is now applied to simulations at a wide range of NaCl concentrations from 0.5 m to 5 m. Figure 9 shows the radial distribution functions of $\text{Na}^+–\text{Cl}^-$, $\text{Na}^+–\text{Na}^+$, and $\text{Cl}^-–\text{Cl}^-$ in explicit, “implicit $\epsilon(c)$ ”, and “RDF-refined” implicit solvent simulations at 1 m, 3 m, and 5 m. It shows that at 3 m, all of the ion–ion RDFs in the “RDF-refined” model reproduce the corresponding RDF at the atomistic explicit solvent level very well. At 5 m, the “RDF-refined” model still underestimates the first peak of the $\text{Na}^+–\text{Na}^+$ RDF and overestimates the first peak of the $\text{Cl}^-–\text{Cl}^-$ RDF, but the electrolyte structure has improved a lot. However, at 1 m, the first peak of the $\text{Na}^+–\text{Na}^+$ RDF is now overestimated. The first peak of the $\text{Cl}^-–\text{Cl}^-$ RDF is also underestimated, and the agreement with the explicit solvent reference has become worse compared to that with the “implicit $\epsilon(c)$ ” model. This means that by enforcing structural agreement at a specific high ion concentration, we have “lost” transferability to low concentrations. Table 2 also shows the osmotic coefficients obtained with the “RDF-refined” model at 0.5, 1, 3, and 5 m. With great improvement of the electrolyte structure at 3 m, the osmotic coefficient also improves considerably at 3 m. In general, the osmotic coefficients of the “RDF-refined” model are lower than the one of the “implicit $\epsilon(c)$ ” model, thus in better agreement with atomistic reference data. However, we see in Figure 9 that this does not imply better structural agreement at all concentrations. These results show that in our electrolyte systems the effective potentials optimized with one iteration at one specific concentration/state point are not very well transferable to other concentrations/state points. Thus, if one aims at a well-structured electrolyte solution at a very high concentration obtained with an implicit solvent model, one has to apply the correction (possibly with more than one iteration step) at each concentration individually. Even though this contradicts the initial intention to have one model that is transferable to the entire range of concentrations this approach nevertheless has one advantage compared to “traditional” iterative Boltzmann inversion: instead of starting the iterative process individually at each concentration, here all potentials are based on the same set of pair PMFs obtained at infinite dilution and thus systematically related. The iterations apply just a minor correction to these effective potentials. This could be an advantage in complex systems with many different interactions where in principle structure-based methods should converge to a unique solution.⁴⁵ In practice, however, convergence problems are quite common, and the initial guess and the exact method used can influence the set of potentials obtained finally.^{5,20,46}

4. CONCLUSIONS

Transferability to different state points remains an ongoing challenge in the development of reduced-resolution (coarse grained or implicit solvent) simulation models. While effective potentials for hydrophobic entities in aqueous solution parameterized at “infinite” dilution are transferable over a wide range of mixture compositions,²² interactions between charged molecules cannot be immediately transferred to higher concentrations since the ion concentration affects the solvent, leading to different dielectric properties. In the present paper, we have investigated how effective implicit solvent potentials for ions in aqueous solution can be made transferable to a wide range of ion concentrations in a way that both the osmotic behavior and

the electrolyte structure of atomistic, explicit solvent reference simulations are reproduced.

We have studied concentration-dependent effective ion potentials parametrized on the basis of ion–ion pair potentials of mean force at infinite dilution in explicit solvent simulations which are split into a short range (ion-specific, not concentration-dependent) and a long range (electrostatic, with a concentration-dependent dielectric permittivity).^{28,29} As shown previously by Hess et al., these potentials are transferable over a certain range of concentrations and reproduce experimental osmotic coefficients well. In the present paper, we studied more closely the contributions of long-range and short-range parts of the effective interactions to osmotic behavior and electrolyte structure to gain a better understanding between thermodynamic and structural properties obtained with these effective potentials and their transferability within an even wider range of concentrations, up to 5 m.

We observe that the use of a concentration-dependent dielectric constant drastically improves the correspondence of the pair structure in the implicit solvent model with the explicit solvent reference compared to using the higher dielectric permittivity of pure water (at the same time also bringing the osmotic coefficients closer). By making small “artificial” variations to the effective potentials (within the error bars of the initial potential of mean force calculation), we could also show that, even though the osmotic coefficient is intimately linked to the electrolyte structure and can be reproduced by a structure-based (i.e., pair-PMF based) implicit solvent model, it is very sensitive to variations in the PMF, making it difficult to judge the quality of a reduced resolution model solely on the basis of this thermodynamic property. It is even possible to generate three (or more) implicit solvent models out of which two show essentially the same osmotic behavior for very different reasons (and with different electrolyte structures), while two others more or less exhibit the same structure (in good agreement with the explicit solvent reference) but a large variation in osmotic coefficients. This shows that reproducing electrolyte structure and a related thermodynamic property such as the osmotic coefficient may depend differently on different aspects of the interaction potential, namely, the short-ranged attraction in the different minima of V_{short} versus the overall attraction, which is dominated by the tail of the potentials (mainly electrostatic interaction). This is an important observation in the context of transferability of reduced resolution models since the aim of a well transferable model is often not in perfect agreement with a reference at a single state point but in rather reasonable agreement (both structurally and thermodynamically) for a range of state points. Our results show that this can in principle be achieved without entirely sacrificing structural agreement.

At very high concentrations, multi-ion correlations start to play a role in addition to the changed solvent behavior. These effects are by construction not accounted for by the infinite dilution pair potential (based on two ions) and the concentration-dependent dielectric permittivity (which only covers the concentration effect on solvent properties). After analyzing the explicit-solvent electrolyte structure at high ion concentrations, we employed two methods to make the effective ion potentials even further transferable: in a first approach, we reduced the repulsion between like-charged ion pairs at high concentrations (“PMF scaling”). The need to do this can be explained from the fact that the first peak of like-charged ion pair correlation functions in explicit solvent simulations is higher than one

would expect due to electrostatic repulsion in water with reduced dielectric screening. Thus, electrostatic repulsion is counterbalanced by other effects in the system (for example, bridging by additional counterions or specific water molecules), which need to be at least approximately accounted for. The model with reduced dielectric repulsion can be parametrized to reproduce atomistic osmotic coefficients and gives a reasonable representation of electrolyte structure also at very high ion concentrations. Contrasting this rather “thermodynamic property-based” route, we also followed a “structure-based” approach where we apply a single refinement step of the implicit solvent ion potentials targeting the electrolyte structure at one concentration (e.g., 3 m). Such a procedure results in a set of interaction functions for all ion pairs which give a very good representation of the electrolyte structure at this particular concentration and also yield a better agreement in the osmotic coefficient. However, these structurally refined potentials are not highly transferable (only to very small variations in the concentration). That means one would have to apply the refining procedure individually at different concentrations and would obtain a family of interaction potentials which are related since they rely on the same initial infinite dilution pair PMFs.

The present paper illustrates the difficulty to parametrize a transferable reduced resolution model for aqueous electrolyte solutions, especially if one aims at both good structural and good thermodynamic agreement with an explicit solvent reference system up to very high salt concentrations. It, however, also shows that it is possible to obtain a well transferable model by not adhering to a strictly “thermodynamics-based” or “structure-based” route but instead employing elements of both approaches—basing the interactions on the pair structure at infinite dilution and making it transferable to higher concentrations with thermodynamically justified scaling constants.

■ ASSOCIATED CONTENT

S Supporting Information. Additional data are shown concerning (i) the radial distribution functions (RDFs) of all ion pairs computed with effective potentials using the error estimate of the potentials of mean force, (ii) the coordination numbers of the like-charged ion pairs, and (iii) the Kirkwood–Buff integrals of the system. This material is available free of charge via the Internet at <http://pubs.acs.org>.

■ AUTHOR INFORMATION

Corresponding Author

*E-mail: peter@mpip-mainz.mpg.de.

■ ACKNOWLEDGMENT

We would like to thank Biswaroop Mukherjee, Christoph Junghans, and Kurt Kremer for many helpful discussions and Pim Schravendijk for helping to implement the explicit solvent osmotic coefficient calculations. This project has been carried out as part of the priority program SPP 1420 by the German Science Foundation. C.P. gratefully acknowledges financial support by the German Science Foundation within the Emmy Noether program (grant PE 1625/1-1).

■ REFERENCES

- (1) *Coarse-Graining of Condensed Phase and Biomolecular Systems*; Voth, G., Ed.; Chapman and Hall/CRC Press, Taylor and Francis Group: New York, 2008.
- (2) Tschope, W.; Kremer, K.; Batoulis, J.; Burger, T.; Hahn, O. *Acta Polym.* **1998**, *49*, 61–74.
- (3) Müller-Plathe, F. *ChemPhysChem* **2002**, *3*, 754–769.
- (4) Murtola, T.; Bunker, A.; Vattulainen, I.; Deserno, M.; Karttunen, M. *Phys. Chem. Chem. Phys.* **2009**, *11*, 1869–1892.
- (5) Rühle, V.; Junghans, C.; Lukyanov, A.; Kremer, K.; Andrienko, D. *J. Chem. Theory Comput.* **2009**, *5*, 3211–3223.
- (6) Peter, C.; Kremer, K. *Faraday Discuss.* **2010**, *144*, 9–24.
- (7) Nielsen, S. O.; Lopez, C. F.; Srinivas, G.; Klein, M. L. *J. Chem. Phys.* **2003**, *119*, 7043–7049.
- (8) Marrink, S. J.; de Vries, A. H.; Mark, A. E. *J. Phys. Chem. B* **2004**, *108*, 750–760.
- (9) Bond, P. J.; Sansom, M. S. P. *J. Am. Chem. Soc.* **2006**, *128*, 2697–2704.
- (10) Shinoda, W.; Devane, R.; Klein, M. L. *Mol. Simul.* **2007**, *33*, 27–36.
- (11) Michel, J.; Orsi, M.; Essex, J. W. *J. Phys. Chem. B* **2008**, *112*, 657–660.
- (12) Lyubartsev, A. P.; Laaksonen, A. *Phys. Rev. E* **1995**, *52*, 3730–3737.
- (13) Harmandaris, V. A.; Reith, D.; van der Vegt, N. F. A.; Kremer, K. *Macromol. Chem. Phys.* **2007**, *208*, 2109–2120.
- (14) Peter, C.; Delle Site, L.; Kremer, K. *Soft Matter* **2008**, *4*, 859–869.
- (15) Fritz, D.; Harmandaris, V. A.; Kremer, K.; van der Vegt, N. F. A. *Macromolecules* **2009**, *42*, 7579–7588.
- (16) Villa, A.; Peter, C.; van der Vegt, N. F. A. *Phys. Chem. Chem. Phys.* **2009**, *11*, 2077–2086.
- (17) Izvekov, S.; Voth, G. A. *J. Phys. Chem. B* **2005**, *109*, 2469–2473.
- (18) Zhou, J.; Thorpe, I. F.; Izvekov, S.; Voth, G. A. *Biophys. J.* **2007**, *92*, 4289–4303.
- (19) Mullinax, J.; Noid, W. G. *J. Chem. Phys.* **2009**, *131*, 104110.
- (20) Johnson, M. E.; Head-Gordon, T.; Louis, A. A. *J. Chem. Phys.* **2007**, *126*, 144509.
- (21) Allen, E. C.; Rutledge, G. C. *J. Chem. Phys.* **2008**, *128*, 154115.
- (22) Villa, A.; Peter, C.; van der Vegt, N. F. A. *J. Chem. Theory Comput.* **2010**, *6*, 2434–2444.
- (23) Silbermann, J.; Klapp, S. H. L.; Schoen, M.; Chennamsetty, N.; Bock, H.; Gubbins, K. E. *J. Chem. Phys.* **2006**, *124*, 074105.
- (24) Fischer, J.; Paschek, D.; Geiger, A.; Sadowski, G. *J. Phys. Chem. B* **2008**, *112*, 13561–13571.
- (25) Allen, E. C.; Rutledge, G. C. *J. Chem. Phys.* **2009**, *130*, 034904.
- (26) Ghosh, J.; Faller, R. *Mol. Simul.* **2007**, *33*, 759–767.
- (27) Mognetti, B. M.; Virnau, P.; Yelash, L.; Paul, W.; Binder, K.; Müller, M.; MacDowell, L. G. *J. Chem. Phys.* **2009**, *130*, 044101.
- (28) Hess, B.; Holm, C.; van der Vegt, N. F. A. *Phys. Rev. Lett.* **2006**, *96*, 147801.
- (29) Hess, B.; Holm, C.; van der Vegt, N. F. A. *J. Chem. Phys.* **2006**, *124*, 164509.
- (30) Kalcher, I.; Dzubiella, J. *J. Chem. Phys.* **2009**, *130*, 134507.
- (31) Lyubartsev, A. P.; Laaksonen, A. *Phys. Rev. E* **1997**, *55*, 5689–5696.
- (32) Luo, Y.; Roux, B. *J. Phys. Chem. Lett.* **2010**, *1*, 183–189.
- (33) Martínez, L.; Andrade, R.; Birgin, E. G.; Martínez, J. M. *J. Comput. Chem.* **2009**, *30*, 2157–2164.
- (34) Hess, B.; Bekker, H.; Berendsen, H. J. C.; Fraaije, J. G. E. M. *J. Comput. Chem.* **1997**, *18*, 1463–1472.
- (35) Neumann, M. *Mol. Phys.* **1983**, *50*, 841–845.
- (36) van der Spoel, D.; Lindahl, E.; Hess, B.; Groenhof, G.; Mark, A. E.; Berendsen, H. J. C. *J. Comput. Chem.* **2005**, *26*, 1701–1718.
- (37) Berendsen, H. J. C.; Postma, J. P. M.; van Gunsteren, W. F.; DiNola, A.; Haak, J. R. *J. Chem. Phys.* **1984**, *81*, 3684–3690.
- (38) Essmann, U.; Perera, L.; Berkowitz, M. L.; Darden, T.; Lee, H.; Pedersen, L. G. *J. Chem. Phys.* **1995**, *103*, 8577–8593.
- (39) Miyamoto, S.; Kollman, P. A. *J. Comput. Chem.* **1992**, *13*, 952–962.
- (40) Weerasinghe, S.; Smith, P. E. *J. Chem. Phys.* **2003**, *119*, 11342–11349.
- (41) Robinson, R. A.; Stokes, R. H. *Trans. Faraday Soc.* **1949**, *45*, 612–624.
- (42) Hess, B.; van der Vegt, N. F. A. *Proc. Natl. Acad. Sci. U. S. A.* **2009**, *106*, 13296–13300.
- (43) Pitzer, K. S.; Mayorga, G. *J. Phys. Chem.* **1973**, *77*, 2300–2308.
- (44) Reith, D.; Pütz, M.; Müller-Plathe, F. *J. Comput. Chem.* **2003**, *24*, 1624–1636.
- (45) Henderson, R. L. *Physics Lett. A* **1974**, *49*, 197–198.
- (46) Rzepiela, A. J.; Louhivuori, M.; Peter, C.; Marrink, S. J. *Phys. Chem. Chem. Phys.* [Online] DOI: 10.1039/c0cp02981e.